Model of induction shrink fit between disk and shaft

Ivo Doležel
Czech Technical University
166 27 Praha 6, Technická 2, e-mail: dolezel@fel.cvut.cz

Václav Kotlan, Bohuš Ulrych
University of West Bohemia
306 14 Plzen, Univerzitní 26, e-mail: vkotlan@kte.zcu.cz, ulrych@kte.zcu.cz

A complete proposal of induction shrink fit between a disk and shaft is presented. The proposal consists of two parts. First, a suitable interference between both parts has to be suggested that is be able to transfer the required mechanical torque at a permissible mechanical stress. Then, the process of induction heating of the disk before its putting on the shaft is mapped. The model of the process respecting all nonlinearities is solved numerically in the hard-coupled formulation. The methodology is illustrated with the example of induction shrink fit between the active wheel of gas turbine and shaft.

KEYWORDS: induction shrink fit, magnetic field, temperature field, field of thermoelastic displacements, finite element method, hard coupling.

1. Introduction

Shrink fits between two metal parts are mostly intended for transferring of mechanical forces and torques. From the physical viewpoint, they are based on high elastic stress acting at their contact place. These fits are widely used in numerous industrial and transport applications. Mentioned can be, for example, armature bandages of rotating machines, tires of railway wheels, shrunk-on rings, crankshafts, etc. [1–2]. The process of manufacturing shrink fit by induction heating is shown in Fig. 1.

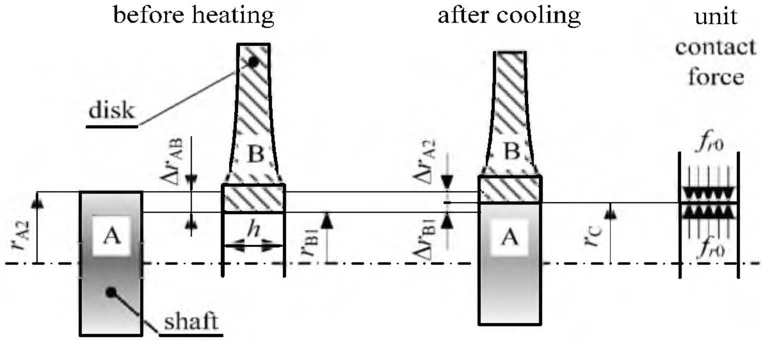

Fig. 1. Realization of induction shrink fit

The shaft of external radius r_{A2} is manufactured with the interference Δr_{AB} with respect to the internal radius r_{B1} of the disk. After heating, the radius of the disk bore must reach a value $r'_{B1} > r_{A2}$ (along the full length of the bore). Putting it on the shaft and cooling, the disk shrinks, which leads to decrease of both radii r_{A2} and r'_{B1} to a common radius r_C that satisfies inequality $r_{B1} < r_C < r_{A2}$ (in our considerations even the shaft is supposed to be elastic). Shrinking of both parts produces (at the place of their contact) a unit force $\pm f_{r0}$ (index 0 means "at rest") between them (see Fig. 1), which allows transferring the mechanical torque.

2. Description of technical problem

Suppose that both disk and shaft are made of the same material. The fit must be able to transfer a prescribed mechanical torque $M_{n_0 \max}$ at the known nominal revolutions n_0. The task is to propose the principal parameters of the fit and check them with respect to all operational viewpoints. The complete model of the problem consists of the following sub-models:

- Starting from the geometry of the disk and given torque $M_{n_0 \max}$, first it is necessary to find an appropriate interference Δr_{AB}. The simplest way is to find the dependence $M_{n \max}(\Delta r_{AB})$ ($M_{n \max}$ being the maximum transferable torque for the given interference Δr_{AB} and revolutions n ranging from 0 to n_0) and then to estimate the value Δr_{AB} from this curve.
- Check of the mechanical stress in the disk after its pressing on the shaft, which starts from knowledge of the unit force $\pm f_{rn}$ acting along their mutual contact for the whole range of possible revolutions $n \in \langle 0, n_0 \rangle$. This value then serves for computing the reduced stress σ_{red} that is then compared with the yield stress σ_y of the steel used (there must hold $\sigma_{red} < \sigma_y$).
- Mapping of the process of induction heating of the disk. Its purpose is to find the parameters of the field current in the inductors (amplitude and frequency) that would secure that the internal radius of the disk reaches a value r'_{B1} in a reasonable time, still acceptable temperature and a good efficiency.

3. Continuous mathematical model

The mathematical model of the task consists of two independent sub-models. The first of them is purely mechanical and its goal is to find the unit contact force $\pm f_{rn}$ acting along the contact place after pressing for the considered range of revolutions $n \in \langle 0, n_0 \rangle$, corresponding to maximum transferable torques $M_{n\max}$, and reduced stress σ_{red}. If these results are acceptable, another sub-model for the description of the process of induction heating is applied.

As the arrangement of the system is practically axi-symmetric, the task can be formulated in the co-ordinates r and z. The first mechanical sub-model is given by the isothermic Lamé equation in the form [3]

$$(\varphi+\psi)\cdot \operatorname{grad}(\operatorname{div}\boldsymbol{u})+\psi\cdot\Delta\boldsymbol{u}+\boldsymbol{f}_{\text{L}}=\boldsymbol{0},$$
$$\varphi=\frac{\nu\cdot E}{(1+\nu)(1-2\nu)},\ \psi=\frac{E}{2\cdot(1+\nu)}. \tag{1}$$

Here, E denotes the Young modulus of elasticity, ν is the Poisson coefficient of the contraction, symbol $\boldsymbol{u}=(u_r, u_z)$ represents the vector of the displacements, and $\boldsymbol{f}_{\text{L}}=(f_{\text{L},r}, f_{\text{L},z})$ stands for the vector of the volumetric forces. While $f_{\text{L,z}}=0$, the component $f_{\text{L},r}$ is given by the formula for the specific centrifugal force

$$f_{\text{L},r}=\rho r\omega^2,\quad \omega=2\pi n/60, \tag{2}$$

where ρ denotes the specific mass of material of the disk.

As the unit contact force f_{rn} is not known beforehand, the task must be solved iteratively. After finishing this iterative process, we can easily find the maximum transferable torque $M_{n\max}$ and also the reduced stress (in our case von Mises stress $\sigma_{\text{red},n\text{Mi}}$). The relation for the torque $M_{n\max}$ reads

$$M_{n\max}=2\pi r_{\text{C}}^2 h\left|f_{rn}\right|f_{\text{f}},\quad r_{\text{C}}=r_{\text{B1}}+\Delta r_{\text{B1}}, \tag{3}$$

where h denotes the length of the bore of the disk (Fig. 1), r_{C} stands for the final common radius of the shaft and disk, and f_{f} is the coefficient of dry friction steel – steel. The von Mises reduced stress $\sigma_{\text{red},n\text{Mi}}$ is given by the formula

$$\sigma_{\text{red},n\text{Mi}}=\sqrt{\frac{1}{2}\left[(\sigma_r-\sigma_z)^2+\sigma_r^2+\sigma_z^2\right]}, \tag{4}$$

where σ_r and σ_z denote the radial and axial stresses at a point, respectively.

The second sub-model describing the process of induction heating consists of three partial differential equations describing the distribution of the magnetic field, temperature field an field of thermoelastic displacements.

Magnetic field in the system is described by the solution of a well-known parabolic equation for magnetic vector potential A in the form [4]

$$\operatorname{curl}\left(\frac{1}{\mu}\operatorname{curl}A\right)+\gamma\frac{\partial A}{\partial t}=\boldsymbol{J}_{\text{ext}}, \tag{5}$$

where μ denotes the magnetic permeability, γ stands for the electric conductivity and $\boldsymbol{J}_{\mathrm{ext}}$ is the vector of the external harmonic current density in the field coils.

But solution to (5) is, in this particular case, practically unfeasible. The reason consists in the deep disproportion between the frequency f (usually tens or hundreds Hz) of the field current I_{ext} and time of heating t_{H} (several minutes). That is why the model was somewhat simplified using the assumption that the magnetic field is harmonic. In such a case it can be described by the Helmholtz equation for the phasor $\underline{A}$ of the magnetic vector potential A [4]

$$\mathrm{curl}\left(\mathrm{curl}\underline{A}\right) + \mathrm{j} \cdot \omega\gamma\mu\underline{A} = \mu\underline{\boldsymbol{J}}_{\mathrm{ext}} . \tag{6}$$

Here, ω denotes the angular frequency ($\omega = 2\pi f$). But the magnetic permeability of ferromagnetic parts is not supposed to be a constant; its value is always assigned to the local value of magnetic flux density $\boldsymbol{B}$. It computation is, in such a case, based on an appropriate iterative procedure.

The temperature field is described by the heat transfer equation [5]

$$\mathrm{div}\left(\lambda \cdot \mathrm{grad}T\right) = \rho c_{\mathrm{p}} \cdot \frac{\partial T}{\partial t} - p , \tag{7}$$

where λ is the thermal conductivity, ρ denotes the mass density and c_{p} stands for the specific heat (all of these parameters are generally temperature-dependent functions). Finally, symbol p denotes the time average internal volumetric sources of heat that generally consist of the volumetric Joule and magnetization losses.

Finally, the solution of the thermoelastic problem is solved by means of the Lamé non-isothermic equation in the form [3]

$$\left(\varphi + \psi\right) \cdot \mathrm{grad}\left(\mathrm{div}\,\boldsymbol{u}\right) + \psi \cdot \Delta\boldsymbol{u} - \left(3\varphi + 2\psi\right) \cdot \alpha_{\mathrm{T}} \cdot \mathrm{grad}\,T = \mathbf{0}, \tag{8}$$

where α_{T} is the coefficient of the linear thermal dilatability of material. Other parameters are identical with those in (1).

It is important to notice that practically all physical parameters of material of the disk (μ, γ, λ, ρc_{p}, α_{T}) are generally temperature-dependent functions. That is why the problem characterized by the interaction of the above three fields cannot be solved in the weak formulation. On the other hand, when the temperature of the disk does not exceed about $350\,^{\circ}\mathrm{C}$, the magnetic permeability of steel can be considered independent of temperature.

4. Numerical solution

The numerical processing of the problem was realized by codes QuickField (mechanical sub-model) and COMSOL Multiphysics (mapping of induction heating). The available algorithms were supplemented with a number of own procedures and scripts and some results were verified by computation using our own code Agros2d based on the fully adaptive higher-order finite element method.

Attention was particularly paid to the convergence of results in the dependence on the density of discretization mesh and distance of the artificial boundary (in case of magnetic field), because the results were required to reach 2–3 valid digits.

The mechanical sub-model was solved by the finite element method using the linear elements for the whole range of revolutions. Reaching the above accuracy required a relatively uniform mesh with about 90.000 elements and the system of equations was characterized by a similar number of the degrees of freedom (DOFs).

The problem of induction heating was also solved by the finite element method in the monolithic formulation (with one stiffness matrix), using the quadratic elements for all discretization meshes. The numbers of elements were about 100.000 for magnetic field and about 40.000 for temperature field and field of thermoelastic displacements. The total number of DOFs was about 500.000.

The complete solution of one variant usually took more than 5 hours on a top-level PC.

5. Illustrative example

The solved arrangement is depicted in Fig. 2 (dimensions given in mm). Both parts (disk and shaft) are manufactured of steel AISI 4130. The interference was chosen (after preliminary computations) $\Delta r_{\mathrm{AB}} = 0.2$ mm.

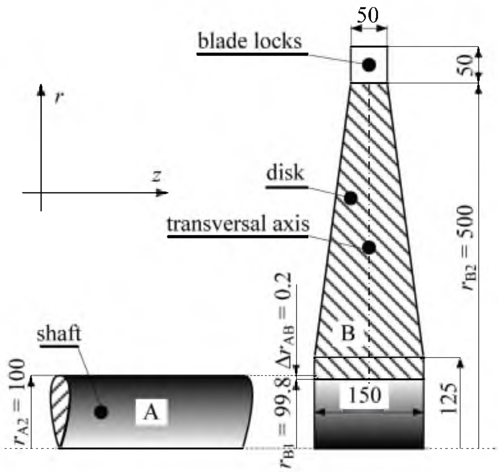

Fig. 2. Basic arrangement of investigated system (dimensions given in mm)

The physical parameters of steel AISI 4130 are known [6]. Some of them (γ, λ, ρ, c_{p}, α_{T}) are temperature-dependent functions, see, for example Figs. 3–5. Other parameters are supposed constant ($E = 2.1\times10^{11}$ N/m^2, $\nu = 0.3$). The yield stress of steel AISI 4130 $\sigma_{\mathrm{y}} = 4.226\times10^{8}$ Nm^{-2} and the coefficient of dry friction steel-steel $f_{\mathrm{f}} = 0.55$.

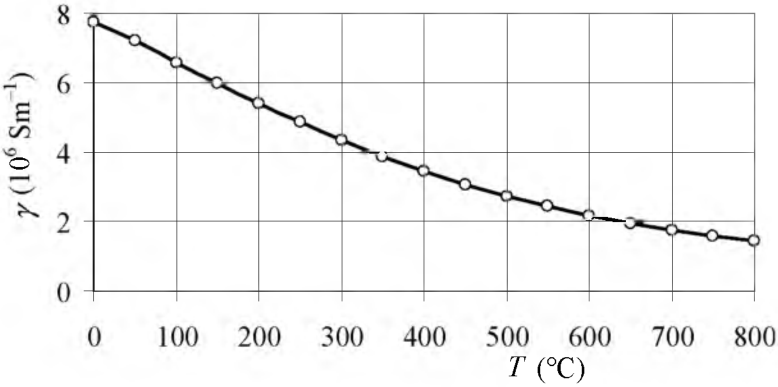

Fig. 3. Steel AISI 4130: electrical conductivity versus temperature

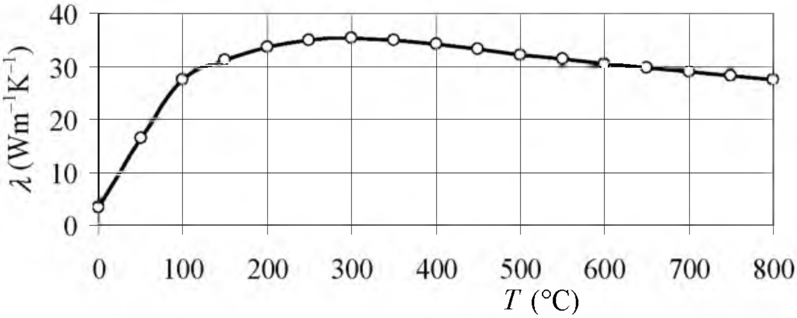

Fig. 4. Steel AISI 4130: thermal conductivity versus temperature

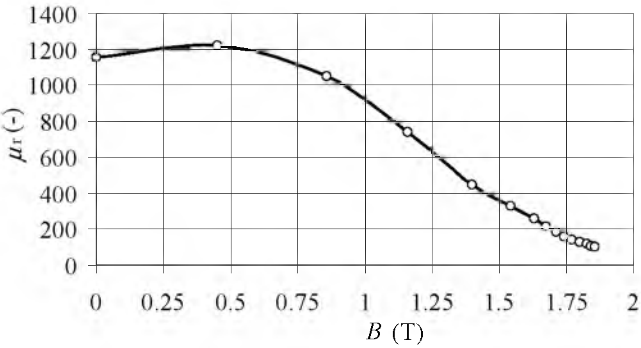

Fig. 5. Steel AISI 4130: relative permeability versus magnetic flux density

The nominal revolutions of the system are $n_0 = 3000\,\text{rpm}$ and power to be transferred $P = 1\,\text{MW}$, i.e., the mechanical torque $M_{n_0} = 3184\,\text{Nm}$.

The most important result of the first sub-model is the distribution of the reduced von Mises stress $\sigma_{\text{red\_Mi}}$ in the disk both at rest and at the nominal revolutions $n_0 = 3000$ rpm. This stress must not exceed the yield stress σ_y. Fig. 6 shows the distributions of $\sigma_{\text{red,Mi}}$ along the transversal axis (see Fig. 2) of the disk.

It is obvious that the highest von Misses stress in the disk occurs (in both regimes) at its internal radius. But as its value is about 3.885×10^8 Nm^{-2}, the fit can be still considered safe. Its higher values for $n_0 = 3000$ rpm are brought about by the stresses produced by the centrifugal forces.

During the process of induction heating the disk is fixed on a ceramic ``shaft'' and heated by two plate-type inductors (see Fig. 6). In order to prevent excessive cooling, the disk is wrapped in a good thermal insulation (glass wool).

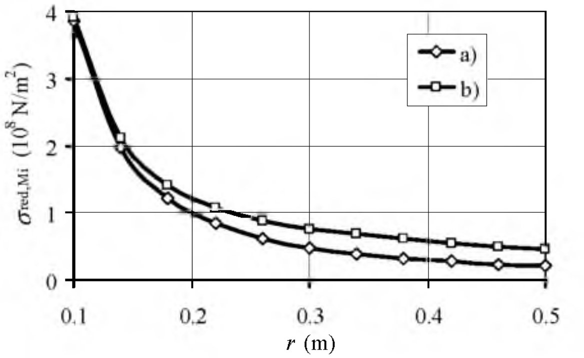

Fig. 6. Distribution of von Mises stress $\sigma_{\text{red,Mi}}$ along the transversal axis of the disk a) after pressing on shaft at rest ($n = 0$) and b) during operation ($n_0 = 3000$ rpm). The force effect of rotating blades is quantified by an additional force $f_{r,\text{B2}} = 8.814 \times 10^7$ Nm^{-2}

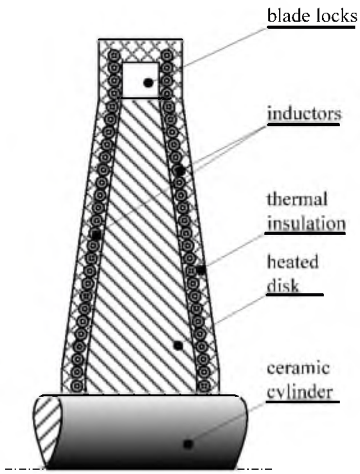

Fig. 7. Arrangement of induction heating

Both inductors with 27 spiral turns made of massive hollow copper conductors cooled by flowing water carry harmonic currents of the same phase shift, thus producing transversal magnetic field in the system. The thermal insulation is placed also in the area of the blade locks. The process of heating is then almost adiabatic, exhibiting a very favorable efficiency.

The field current parameters were selected in accordance with the possibilities of common industrial plants. While its frequency was set $f = 50\,\mathrm{Hz}$, its amplitude ranged from 1–4 kA (such currents are commonly available). The thermal conductivity of high-quality thermal insulation – glass wool – is 0.04 $\mathrm{Wm^{-1}K^{-1}}$ and its specific heat is $0.04824\times10^{6}\,\mathrm{Jm^{-3}K^{-1}}$. The average temperature of the cooling water in the hollow conductors of the inductor $T_{\mathrm{w}} = 50\,^{\circ}\mathrm{C}$ and the initial temperature of the system (including ambient air) before heating $T_0 = 30\,^{\circ}\mathrm{C}$.

Due to poor thermal conductivity of glass wool the boundary conditions along the area containing the disk and inductors placed in thermal insulation are restricted just on convection (coefficient $\alpha = 20\,\mathrm{Wm^{-2}K^{-1}}$).

The most important results are depicted in Figs. 8 and 9. Figure 8 contains the evolution of the average temperatures of the disk in time for different RMS values of the field current ranging from 1 kA to 5 kA.

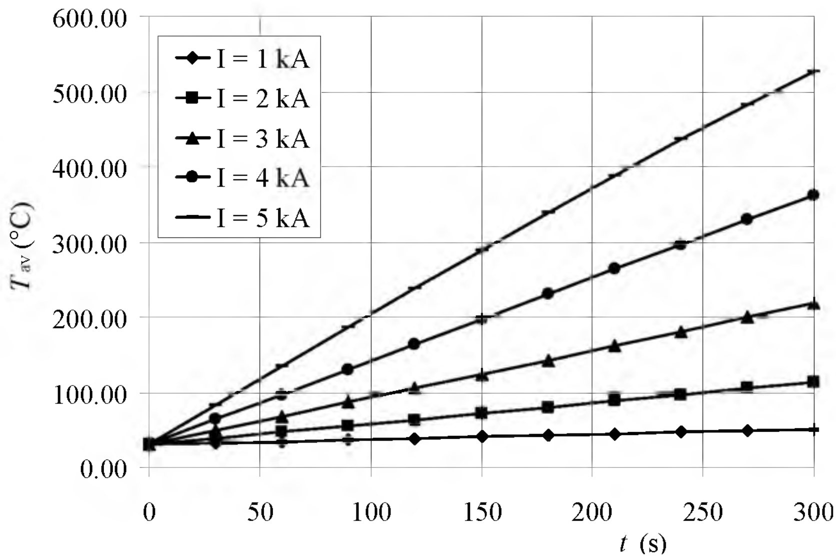

Fig. 8. Time evolution of average temperature of disk for different RMS values of field current

In order to reach the displacement equal to $\Delta r_{\mathrm{AB}} = 0.2$ mm as required in time shorter than 180 s we have to use field currents I of RMS value 4 or 5 kA. In the first case, this displacement in the axis is reached in about 253 s, in the second case in 190 s. But such displacements must appear along the whole length of the bore. The corresponding time evolutions are (for current $I = 4$ kA) depicted in Fig. 9.

Now it is clear that for the field current $I = 4$ kA the displacement u exceeding the prescribed interference $\Delta r_{AB} = 0.2$ mm along the whole length of the bore is reached in about 270 s.

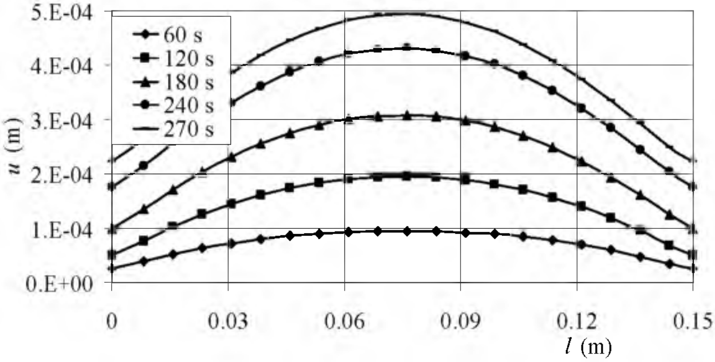

Fig. 9. Time evolution of displacements along the bore of the disk for field current $I = 4$ kA

6. Conclusion

The paper deals with the proposal of an axisymmetric shrink fit. First, a complete continuous mathematical model of the problem is suggested. This model is then solved numerically in two steps: the first one being aimed at mechanical properties of the fit while the second one at mapping of the process of induction heating. The results obtained are physically real and well correspond with the common industrial experience. Nevertheless, we plan (in collaboration with some industrial plant because the realization is beyond the possibilities of academic workshops) their experimental verification.

Nevertheless, even when the methodology is obviously correct and applicable for practice, further research should be aimed at the simplification of its realization. Still, the authors had to combine two-three various codes supplemented with own procedures and scripts. The processing of one variant takes a long time (on a top-level PC it is usually more than 5–6 hours); that is why the acceleration of the algorithms is a must. More attention should also be paid to the accuracy of the input data (temperature dependencies of physical parameters of various materials) because they often exhibit substantial variances pending on their sources (databases, datasheets etc.).

Another direction of research is optimization of the process of heating the disk that is characterized by more degrees of freedom. For example, if the profile of the disk is geometrically nonuniform, uniformly wound inductors do not seem to be the best solution. In order to reach a homogeneous temperature profile in it, the internal turns of the inductors should be wound densely only near the bore. With growing diameter, the distance between particular turns could also grow. Another version is heating of the disk by the complete inductors, but after reaching some prescribed temperature their external parts could be switched off in order to prevent the narrower upper parts of the disk from overheating.

Acknowledgment

This work was financially supported by the Grant project GACR P102/11/0498.

References

[1] P. Pedersen, On Shrink Fit Analysis and Design, Computational Mechanics, Vol. 8, No. 4, pp. 121–130, 2006.
[2] P. Karban, V. Kotlan, and I. Dolezel, Numerical Model of Induction Shrink Fits in Monolithic Formulation, IEEE Trans. Magn. Vol. 48, No. 2, pp. 315–318, 2012.
[3] B. A. Boley and J. H. Weiner, Theory of Thermal Stresses. Dover Publications, 2011.
[4] M. Kuczmann and A. Ivanyi, The Finite Element Method in Magnetics. Akademiai Kiado, Budapest, 2008.
[5] J. P. Holman, Heat Transfer. McGraw-Hill, New York, 2002.
[6] Temperature Dependent Elastic and Thermal Properties Database. Available: http://www.jahm.com.